(12) 6

AD A124057

January 1983 SC5202.20SA

GROWTH OF HgCdTe BY MODIFIED MOLECULAR BEAM EPITAXY

Semi-Annual Technical Report No. 6
For period 03/01/82 through 08/31/82

Contract No. MDA903-79-C-0188
DARPA Order No. 3704

Contract Effective Date: 01/12/79
Contract Expiration Date: 05/31/83

Prepared for:

Defense Advanced Research Projects Agency
1400 Wilson Blvd.
Arlington, VA 22209

DTIC
ELECTE
FEB 3 1983
S D
B

Prepared by:

J. T. Cheung
Principal Investigator
(805) 498-4545, Ext.144

This research was sponsored by the Defense Advanced Research Projects Agency under DARPA Order No. 3704, Contract No. MDA903-79-C-0188; Monitored by Defense Supply Service.

Rockwell International
Science Center

UNCLASSIFIED

SECURITY CLASSIFICATION OF THIS PAGE (When Data Entered)

REPORT DOCUMENTATION PAGE		READ INSTRUCTIONS BEFORE COMPLETING FORM
1. REPORT NUMBER	2. GOVT ACCESSION NO. AD A124057	3. RECIPIENT'S CATALOG NUMBER
4. TITLE (and Subtitle) GROWTH OF HgCdTe BY MODIFIED MOLECULAR BEAM EPITAXY		5. TYPE OF REPORT & PERIOD COVERED Semi-Annual Technical Report 03/01/82 thru 08/31/82
		6. PERFORMING ORG. REPORT NUMBER SC5202.20SA
7. AUTHOR(s) J. T. Cheung H. Sankur		8. CONTRACT OR GRANT NUMBER(s) MDA903-79-C-0188
9. PERFORMING ORGANIZATION NAME AND ADDRESS Rockwell International Science Center 1049 Camino Dos Rios Thousand Oaks, CA 91360		10. PROGRAM ELEMENT, PROJECT, TASK AREA & WORK UNIT NUMBERS DARPA Order No. 3704
11. CONTROLLING OFFICE NAME AND ADDRESS Defense Advanced Research Projects Agency 1400 Wilson Blvd. Arlington, VA 22209		12. REPORT DATE January 3, 1983
		13. NUMBER OF PAGES 37
14. MONITORING AGENCY NAME & ADDRESS (if different from Controlling Office)		15. SECURITY CLASS. (of this report) Unclassified
		15a. DECLASSIFICATION DOWNGRADING SCHEDULE

16. DISTRIBUTION STATEMENT (of this Report)

Approved for public release; distribution unlimited.

17. DISTRIBUTION STATEMENT (of the abstract entered in Block 20, if different from Report)

18. SUPPLEMENTARY NOTES

19. KEY WORDS (Continue on reverse side if necessary and identify by block number)

LADA, HgCdTe, CdTe, GaAs, ZnO, laser evaporation, thin film, Epitaxy, heteroepitaxy

20. ABSTRACT (Continue on reverse side if necessary and identify by block number)

The LADA Technique has been used to grow thin films of HgCdTe, CdTe, and ZnO films on various substrates.

Single crystalline $Hg_{0.7}Cd_{0.3}Te$ films of up to 15 μm thick were deposited on (111) CdTe substrates. Their electrical properties can be improved or altered by post-annealing in Hg over pressure. After annealing at 410°C, the films were successfully converted to p-type. Ion implanted n^+/p photodiodes were demonstrated.

Con't. - over

DD FORM 1 JAN 73 1473

UNCLASSIFIED

SECURITY CLASSIFICATION OF THIS PAGE (When Data Entered)

Heteroepitaxial layers of (111) CdTe with excellent surface morphology were grown on (100) GaAs substrates. Near the interface region, there is a high density of misfit dislocations. However, the crystalline quality improves abruptly at approximately 2 μm from the interface. Dislocation density was determined by TEM analysis. At 6 μm from the interface, it is as low as $10^5/cm^2$.

ZnO films were deposited on a large variety of substrates. The growth condition and mechanism were studied in detail as the function of substrate temperature, ambient condition, annealing condition, and doping. Films with good uniformity and smooth morphology were obtained. They are uniaxially oriented in the (0002) direction and have very high resistivity.

TABLE OF CONTENTS

LIST OF FIGURES

LIST OF TABLES

1.0 INTRODUCTION

1.1 Program Objectives

The main objective of this program is to explore and develop a novel thin film deposition technique, i.e., Laser Assisted Deposition and Annealing (LADA). It will be demonstrated for two materials HgCdTe and ZnO.

1.2 Overall Approach

The program started in February 1979. The work performed during the first phase (1979-1981) exclusively involved HgCdTe.

The second phase started in May, 1981. Deposition of ZnO thin film by laser evaporation was added to the program as a new task. A separate LADA system has been built to deposit ZnO in order to prevent intercontamination between two materials. In this report, the progress on both material developments will be reported.

1.3 Accomplishments

Accomplishments in this period are summarized in the following:

1.3.1 HgCdTe

I. HgCdTe on CdTe:

a. Grown thick (> 15 μm) HgCdTe layers on (111) CdTe substrates.
b. Reduced n-type impurities. Consequently, as-grown layers could be converted to p-type by annealing.
c. Demonstrated n^+/p implanted photodiodes fabricated on LADA grown $Hg_{0.7}Cd_{0.3}Te$ layers.

II. CdTe on Alternative Substrates

a. Carried out preliminary experiments of depositing CdTe on (110) and (100) Si and (100) GaAs. Single crystalline CdTe films were successfully grown on (100) GaAs substrates

b. Confirmed excellent crystallinity of CdTe (111)/GaAs (100) heteroepitaxy by TEM.

1.3.2 ZnO

The information accumulated during this period is derived from over 200 runs. Research efforts were emphasized on optimizing the growth conditions in order to provide materials suitable for SAW device fabrication. Major achievements are:

I. Studied the physics of ZnO evaporation by pulsed CO_2 laser irradiation as well as ZnO desorption mechanisms.

II. Studied the effect on film quality due to substrate temperature, post annealing condition, different substrate and source materials.

III. Improved the electrical properties (i.e., resistivity) by Li-doping and by carrying out the deposition in an oxygen plasma.

2.0 TECHNICAL INFORMATION

This section is divided into two parts: HgCdTe and ZnO.

2.1 HgCdTe

2.1.1 HgCdTe on CdTe

In the course of this work, we have experienced some key problems. First, we were not able to maintain a constant laser power density on the source surface; as a result, the thickness of the films was limited to 10 μm or less. For device fabrication, the minimum requirement is approximately 15 μm. The second problem deals with the generally inferior electrical properties of these films compared to the bulk material. After annealing at 210°C in a Hg over pressure, a layer with χ = 0.3 composition at 77°K exhibited an electron mobility between 10,000 to 19,000 $cm^2/V\text{-}s$ (40% of bulk value) and a carrier concentration around 3-7 × 10^{16} cm^{-3} (two order of magnitude higher than bulk value). They are believed to be caused by a combination of impurity contaminations and native defects. The most peculiar, yet severe, problems were the unsuccessful attempts to convert the as-grown n-type layers to p-type by annealing at 410°C. During this period, some of these problems have been identified and solved. The results will be discussed in the following sections.

2.1.1.1 Growth of Thick HgCdTe Films

Condensation of evaporants onto the vacuum window through which the laser beam transmits caused severe problems. Condensation on the window gradually cuts down its transmittance and reduces the laser power on the source surface. After some build-up, the window can eventually become opaque. Our solution was to reflect the laser beam onto the source surface by a heated mirror. This arrangement enables us to deposit films up to 10 μm thick. The problem is only partially solved because evaporants can bounce from the mirror

surface onto the window. In our recent approach, we have eliminated the mirror. In the new design, constant evaporation rate can be maintained until the source material exhausts. Under 1×10^{-4} Torr of Hg back pressure and 130°C substrate temperature, we are able to maintain a deposition rate of 2.3 μm/hr without Hg loss. Bulk $Hg_{0.7}Cd_{0.3}Te$ ingots from New England Research Center were used as evaporation source. Each ingot of 1" long by 1/2" in diameter can yield six 15 μm thick films.

2.1.1.2 P-Type HgCdTe Layers by LADA

The as-grown films with a composition of $x = 0.3$ are always n-type at 77°K. During the last reporting period (Oct. 1981 to March 1982), their mobility and carrier concentration were 4000-7500 $cm^2/V\text{-}s$ and 7×10^{15}-$3 \times 10^{16} cm^{-3}$, respectively. After annealing at 210°C in Hg over pressure, these values became 10,000-19,000 $cm^2/V\text{-}s$ and $5\text{-}7 \times 10^{16} cm^{-3}$, respectively. However, after annealing under the p-type conversion condition (i.e., 410°C), they remained n-type. The persistency suggests that they were heavily compensated. In the previous semi-annual report (No. 5), we speculated Al and Si being major dopant impurities. After cleaning up the system and eliminating the most likely source for Al and Si, we are now able to grow films which can be converted to p-type by annealing at 410°C.

Figure 1 shows the morphology of such a layer. It is very smooth except for some terracing a few hundred A high. The layer is (111) oriented single crystal as determined by x-ray Laue diffraction shown in Fig. 2. Its mobility and hole concentration at 77K are 138 $cm^2/V\text{-}s$ and 2×10^{16} cm^{-3}, respectively. The carrier concentration is comparable to LPE material, except the mobility is a factor of two lower. Electrical properties of these films measured at 300°K and 77°K are summarized in Table 1. Standard processing was used to fabricate n^+/p implanted photodiodes. The I-V curve and spectral response is shown in Fig. 3. The forward resistance is anomalously high. This is believed to be due to processing rather than to material properties. The

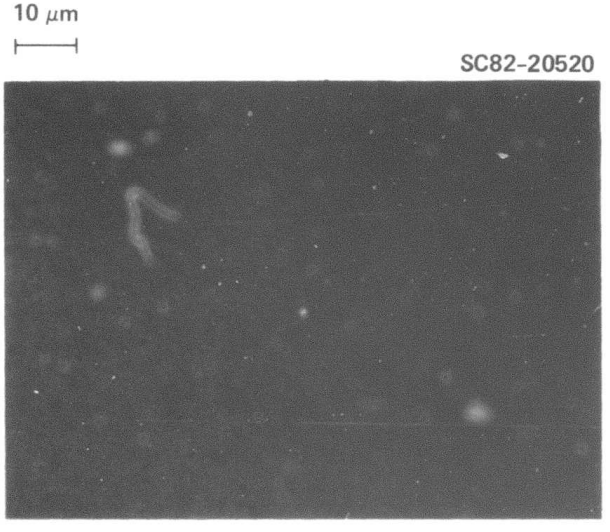

Fig. 1 Morphology of a p-type LADA $Hg_{0.7}Cd_{0.3}Te$ layer.

SC82-19348

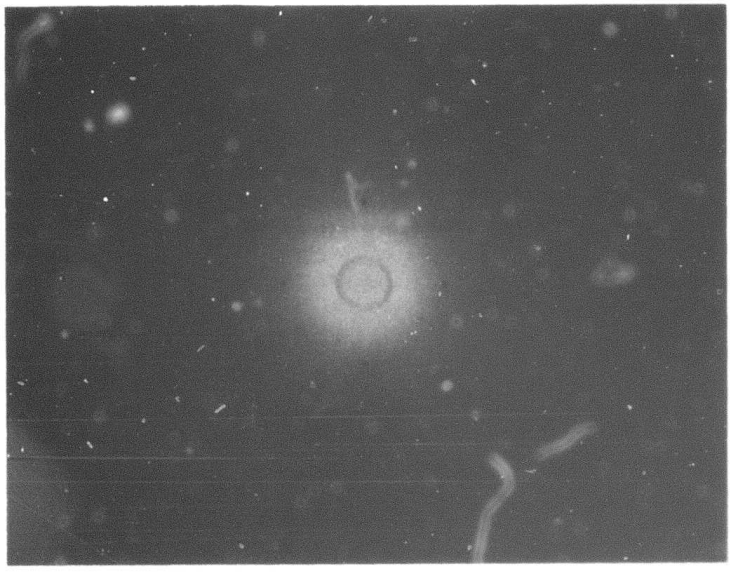

Fig. 2 X-ray Laue diffraction of a LADA $Hg_{0.7}Cd_{0.3}Te$ layer.

SC82-19347

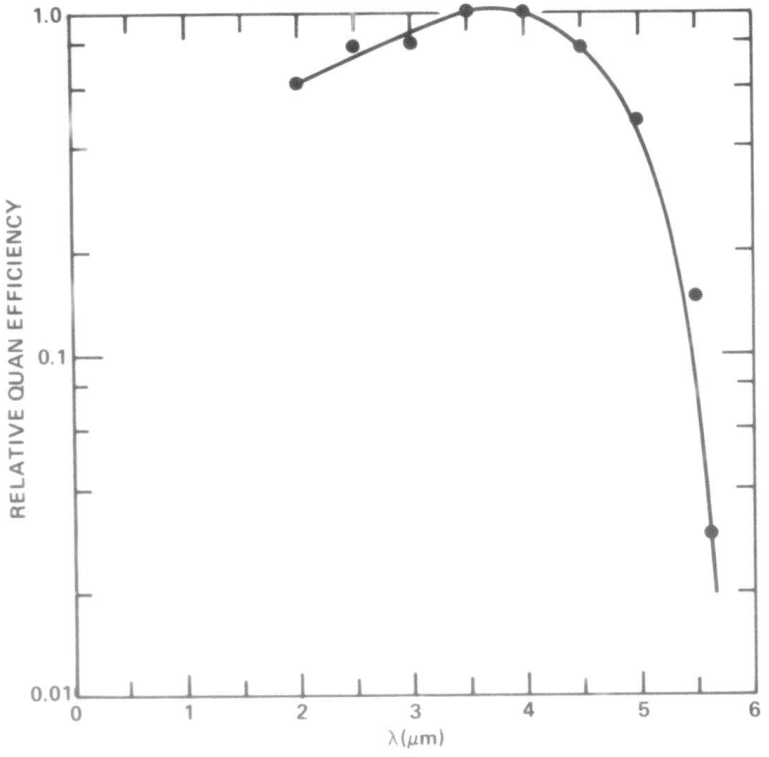

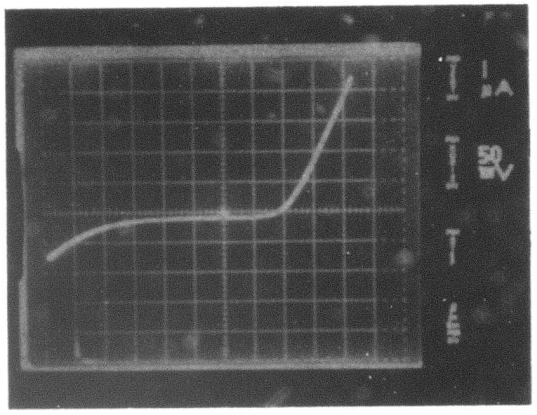

Fig. 3 I-V curve and spectral response of the first n^+/P photodiode fabricated on LADA $Hg_{0.7}Cd_{0.3}Te$.

Rockwell International
Science Center
SC5202.20SA

Table 1

77K Electrical Properties of LADA $Hg_{1-x}Cd_xTe$ Films, As-Grown and After Annealed

Sample No.	Type	Composition (x)	Treatment	~ $cm^2/V\text{-}s$	n(p) cm^{-3}	Remarks
113	n	0.3	As Grown	Not Measurable	Not Measurable	High laser power
	n	0.3	210°C Annealing	7,000	2×10^{16}	
139	n	0.3	As Grown	7,400	1.3×10^{16}	Low laser power
	n	0.3	210° Annealing	11,000	8×10^{16}	
115	n	0.2	As Grown	22,000	3.5×10^{16}	Low laser power
156	p	0.3	410°C annealing	138	2×10^{16}	First p-type

spectral response peaks at 4 μm with (50%) cut-off at 5 μm. The cut-off wavelength indicates a composition of $x = 0.3$ which agrees with the composition of the starting source material. This confirms the congruent evaporation induced by pulsed heating.

2.1.2 CdTe on Alternative Substrates

One of our goals is to grow HgCdTe on substrates other than CdTe. CdTe layers will be used as a buffer. Among a list of substrate materials, GaAs is a good candidate because of its availability, quality, and transmission characteristics. Despite a large lattice mismatch between their lattice constants (CdTe 6.482Å, GaAs 5.652Å) and difference in the relative orientations [(111) CdTe on (100) GaAs], we obtained surprisingly high quality heteroepitaxial growth. This section will describe the results.

A total of ten runs of CdTe on GaAs were made. GaAs substrates were oriented in the (100) direction to within ±0.5°. Both n-type and semi-insulating substrates were used. The substrates were first degreased and etched; they were then placed on the substrate holder and the system was pumped out. After vacuum reached mid 10^{-7} Torr, the GaAs substrates were flash heated for cleaning. Undoped CdTe crystals were used as source. Prior to deposition it was cleaned by scrubbing the surface with a focused laser beam. The substrate temperature at deposition was 350°C. The growth rate could be varied from 1 μm/hr to 12 μm/hr by increasing the laser power. If the substrate surface was not treated uniformly, the grown layer would be a mixture of rough and smooth regions.

Figure 4 shows the morphology of a rough layer. X-ray Laue diffraction study revealed backscattering from the CdTe film as well as the GaAs substrate. The layer orientation is (100). The (100) axes of the layer and the substrate are parallel indicating epitaxial relationship. The resistivity at room temperature is 1.8×10^5 Ω cm. Figure 5 shows the morphology of the smooth region. The resistivity at room temperature exceeds 10^6 Ω cm. The surface is smooth and free of twins. The only observable features are hexagonal hillocks with a density between $5 \times 10^3/cm^2$ to $10^5/cm^2$.

The quality of CdTe on GaAs was also examined by Transmission Electron Microscopy (TEM). Preliminary results indicate a transition region of about 2 μm thick at the interface. This region has a very high density of misfit dislocations as one would expect for a highly lattice mismatched system (Fig. 6). The density of dislocations decreases as the distance from the CdTe/GaAs interface increases. At 6 μm from interface, the defect density reached a plateau value of ~ 10^4-$10^5/cm^2$ which is comparable to the best bulk CdTe material (Fig. 7). Electron diffraction pattern also indicate the

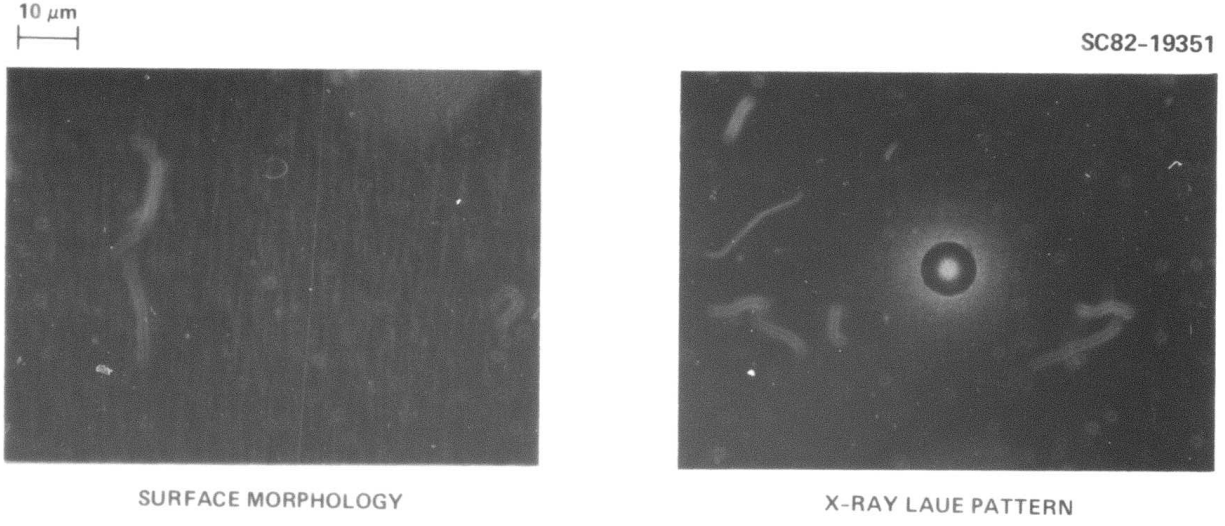

Fig. 4 Morphology and x-ray Laue diffraction of a CdTe (100)/GaAs (100) layer.

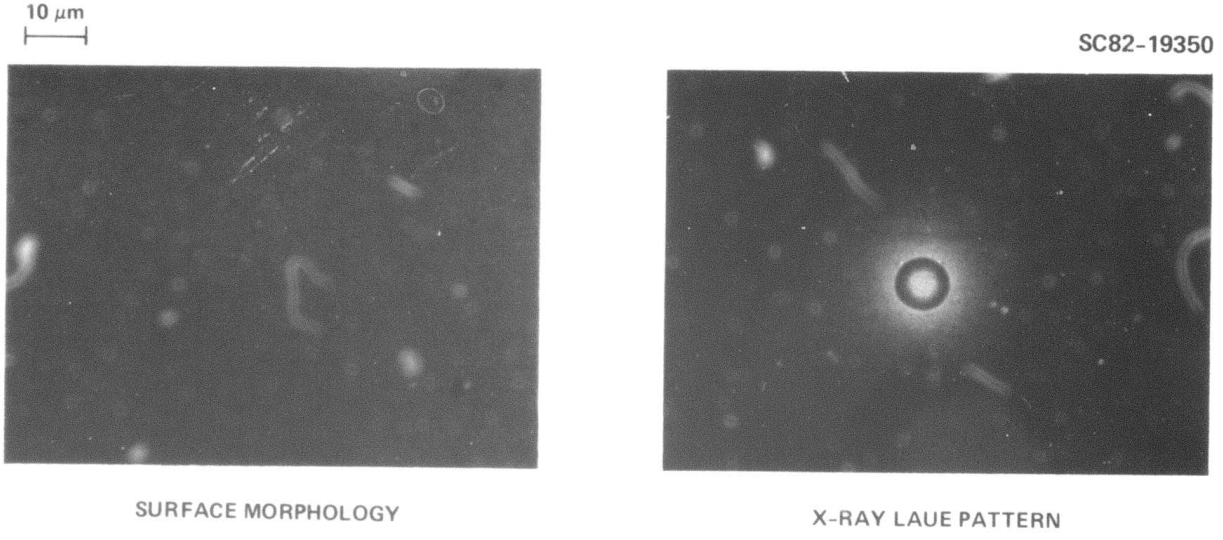

Fig. 5 Morphology and x-ray Laue diffraction of a CdTe (111)/GaAs (100) layer.

SC82-20521

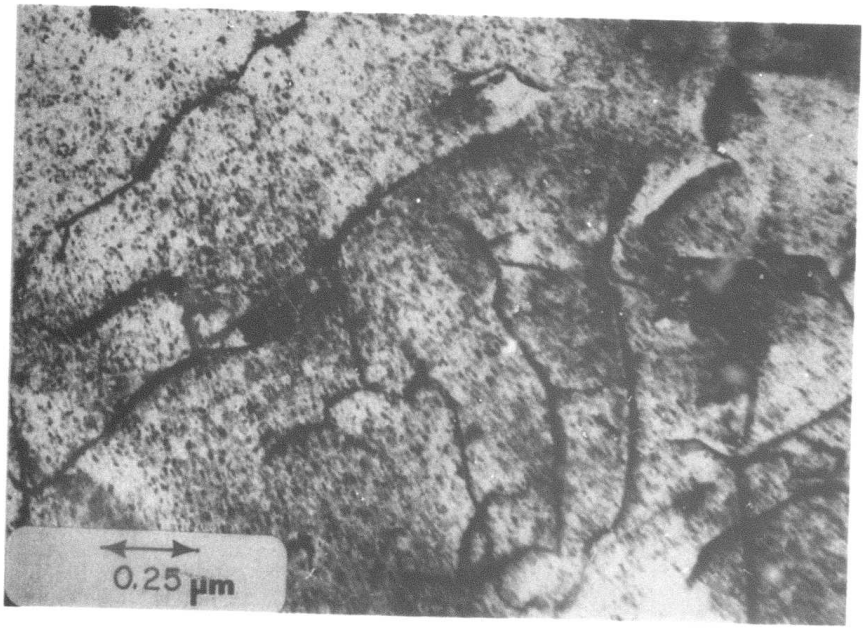

Fig. 6 TEM study of (111) CdTe (111)/GaAs (100). Dislocation lines at the transitional interface region.

SC82-20522

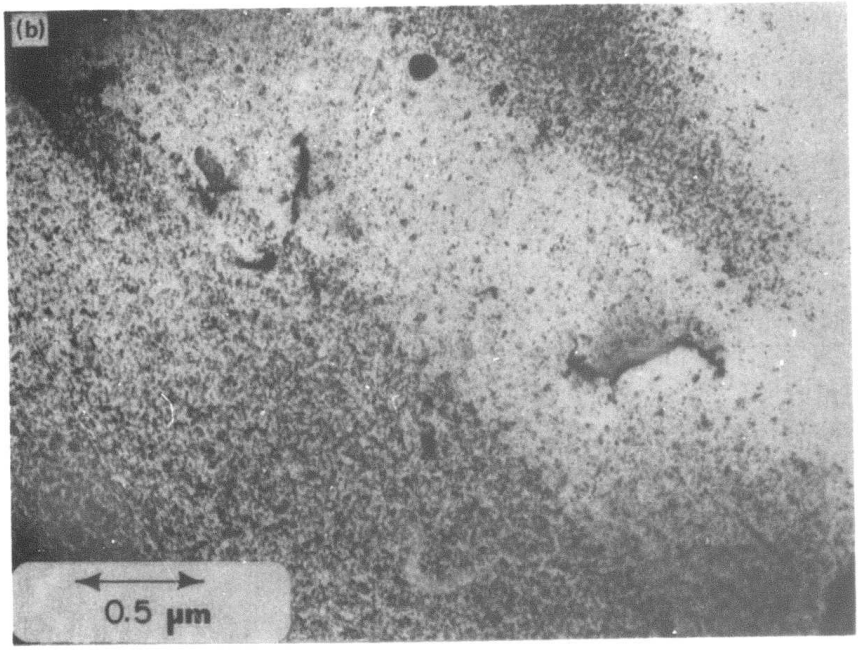

Fig. 7 TEM study of CdTe (111)/GaAs (100). Dislocation lines at 6 μm from the interface.

presence of tellurium precipitates. It may be due to the excess tellurium in the CdTe source. This will be studied with different CdTe source materials. Future collaboration with T. McGee of ARACOR Inc. is planned to study this interesting case of heteroepitaxy. Other characterizations such as photoluminescence, SIMS and UV reflectance analysis are also underway.

2.2 ZnO

In the second half of FY 1982, investigation of laser evaporation and deposition of ZnO has continued, with the main goal of developing this technique to the point where SAW device quality layers can be grown. Below are presented the experimental approach and results.

2.2.1 Experimental

The evaporation apparatus is shown in Fig. 8. It consists of a vacuum chamber and a CO_2 laser. The laser beam is directed inside the vacuum system by scanning mirrors, a ZnSe lens and window. The vacuum system is fitted with IR, visible and UV windows, beam deflecting mirrors, substrate heater, shutter, cold trap, glow discharge electrodes, thickness monitor and ozonizer. A controlled gas back pressure can be maintained in the system by means of hi-vacuum throttling and leak valves. The substrate temperature or bias with respect to electrodes can be varied.

2.2.2 Results

Requirements for SAW device quality ZnO layers are stringent: good crystallinity in the form of single crystal or large size and oriented polycrystals; smooth morphology, to the extent that 2 μ linewidth photolithography can be executed; high resistivity ($\rho > 10^6$ Ω-cm) and high breakdown voltage in order to sustain an RF field across the layer, so that a strain wave can be launched.

In the second half of FY 1982, we have obtained highly oriented ZnO layers on a variety of substrates. These layers have very smooth surface

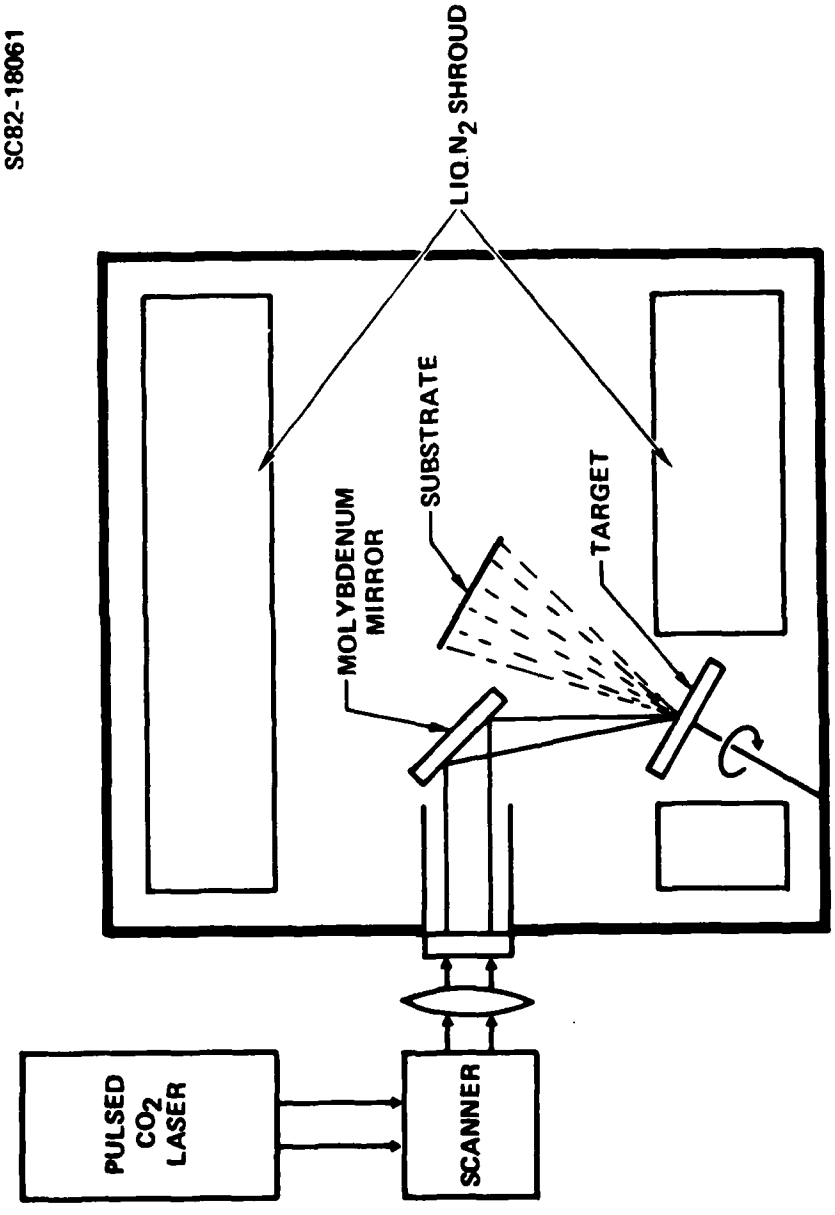

Fig. 8 Laser evaporation apparatus for ZnO.

morphologies, high resistivity and good optical properties. Some high resistivity samples had low breakdown characteristics as grown. However, regions with poor breakdown characteristics, possibly caused by pinholes or defective regions, were found to improve by isothermal annealing. Uniformity over 1 -1/2" diameter area was good within 5% as observed by the interference color of the film and by surface profilometric techniques. In the first part of the next quarter, SAW devices will be made and the electromechanical coupling coefficient measured. Growth conditions and physical parameters of the films are explained below in detail.

1. Effect of ZnO Source Material

Hot pressed pellets purchased from MRC (30-101I-ZN504) and cold pressed pellets prepared in-house with high purity (99.999) ZnO powder were used as evaporation sources. The powder size, the preparation technique - hot or cold pressing - the doping additives were all found to affect the evaporation rate, the amount of laser power required to prevent spitting of particulate material and to obtain good quality films. The quality of the hot pressed pellets varied from batch to batch, therefore, most experiments have been performed using cold pressed pellets made out of powder with reproducible particle size and sintering pressure. Laser evaporation conditions for these in-house samples do not vary nearly as much as those for hot-pressed pellets where factors of two variations in the required laser power have been observed.

2. Physics of ZnO Evaporation

The crystallite size, the packing density of the pellets, the incident laser power all contribute to the evaporation rate, as well as to the phenomenon of spitting of particulate material. The absorption at 10.6 μ by ZnO powder particles will determine the local temperature of the pellet surface, hence the evaporation rate. The absorption is expected to be weak, since the restrahlen absorption band for ZnO occurs at 26 μm, with absorption

peak width of about 10 μm (Fig. 9). In fact, a rough estimate of the absorptivity at 10.6 μm obtained from the ratio of forward and backscattered intensities to the incident laser power, gave values of 20 cm^{-1}. The low thermal conductivity of the powder ZnO (5.8×10^{-5} cal/cm °K sec) causes the heat to be retained in the upper half of the pellet. The spot where the laser beam is focused onto, is heated up to temperatures of about 1000°C, as judged by radiometry. The intense heating probably causes the ZnO to decompose and to evaporate congruently. The calculated vapor pressure of Zn over ZnO and over Zn is shown in Fig. 10. Working back from the evaporation rate, as measured by the loss of pellet weight with time and calculating the vapor pressure of zinc, the temperature of a 100 μm diameter area, the spot size of focused CO_2 laser beam is found to be 900-1200°C, in qualitative agreement with visual observations. The fact that ZnO pellet retains its white color and does not show Zn enrichment at the surface indicated congruent evaporation. Congruent evaporation is achieved even under thermal decomposition of ZnO because of relatively high vapor pressure of Zn for temperatures >800°C. In fact P_{Zn} = 200 Torr at 800°C, p_{Zn} = 1 Atm at 907°C.

The evaporant flux was analyzed by means of a residual gas analyzer. During laser evaporation, oxygen and zinc isotopes signals dominated the RGA spectrum. ZnO signal at 81 amu was comparatively weak, about 1/100-1/1000 of Zn signal.

Zn and ZnO signals were observed to persist up to 1/4 hour, following the turning off of the laser or when a shutter was interposed between RGA and ZnO source. The ZnO signal increased in magnitude when the cold trap was allowed to warm-up releasing such oxidizing species as H_2O, CO, CO_2, O_2. These effects can be accounted by re-evaporation and oxidation of Zn deposited on and around RGA filament. The above observations suggest that ZnO molecular species do not exist in vapor phase and laser evaporation of ZnO target produces Zn and O_2.

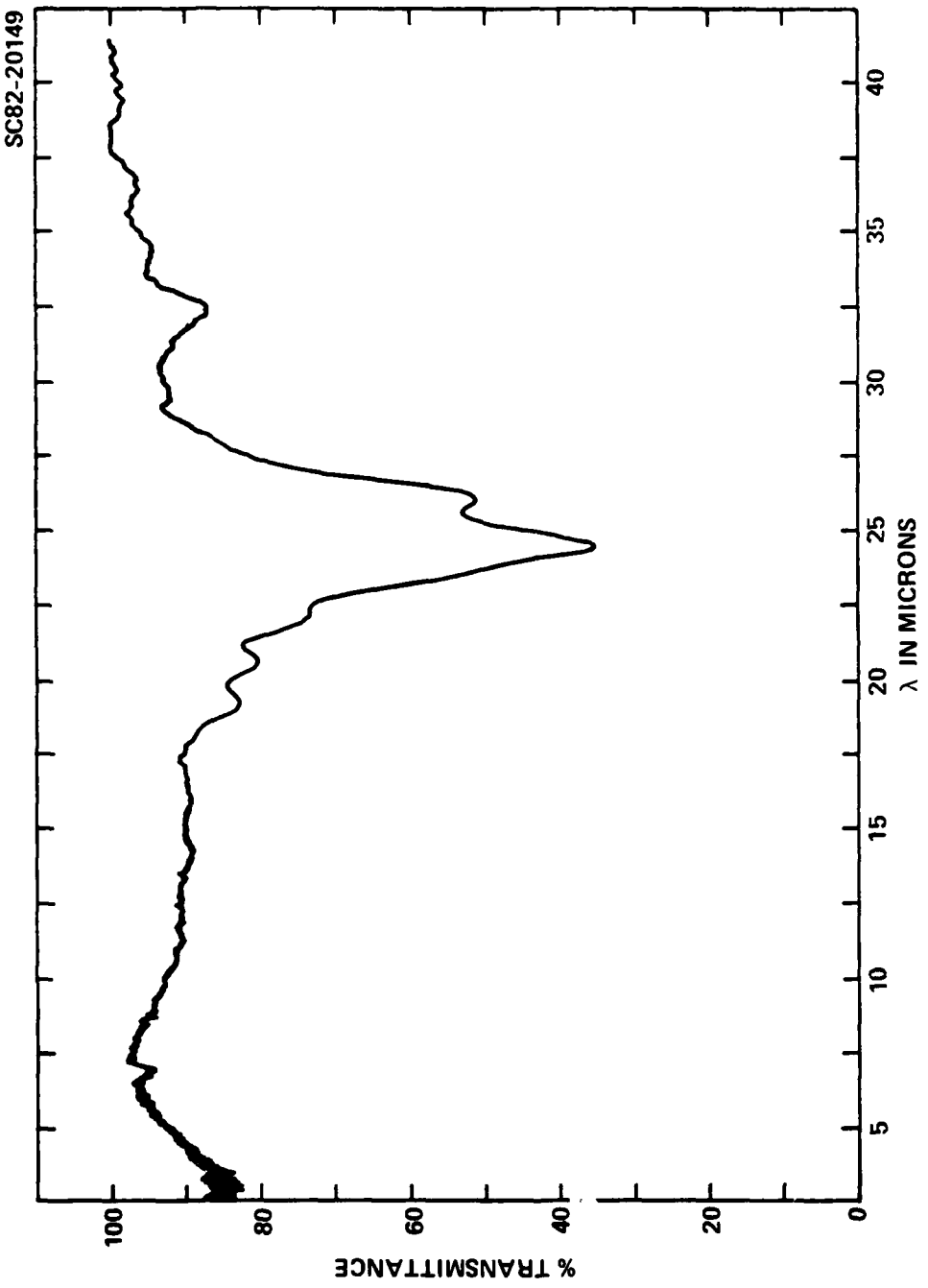

Fig. 9 IR transmission spectrum of a ZnO film.

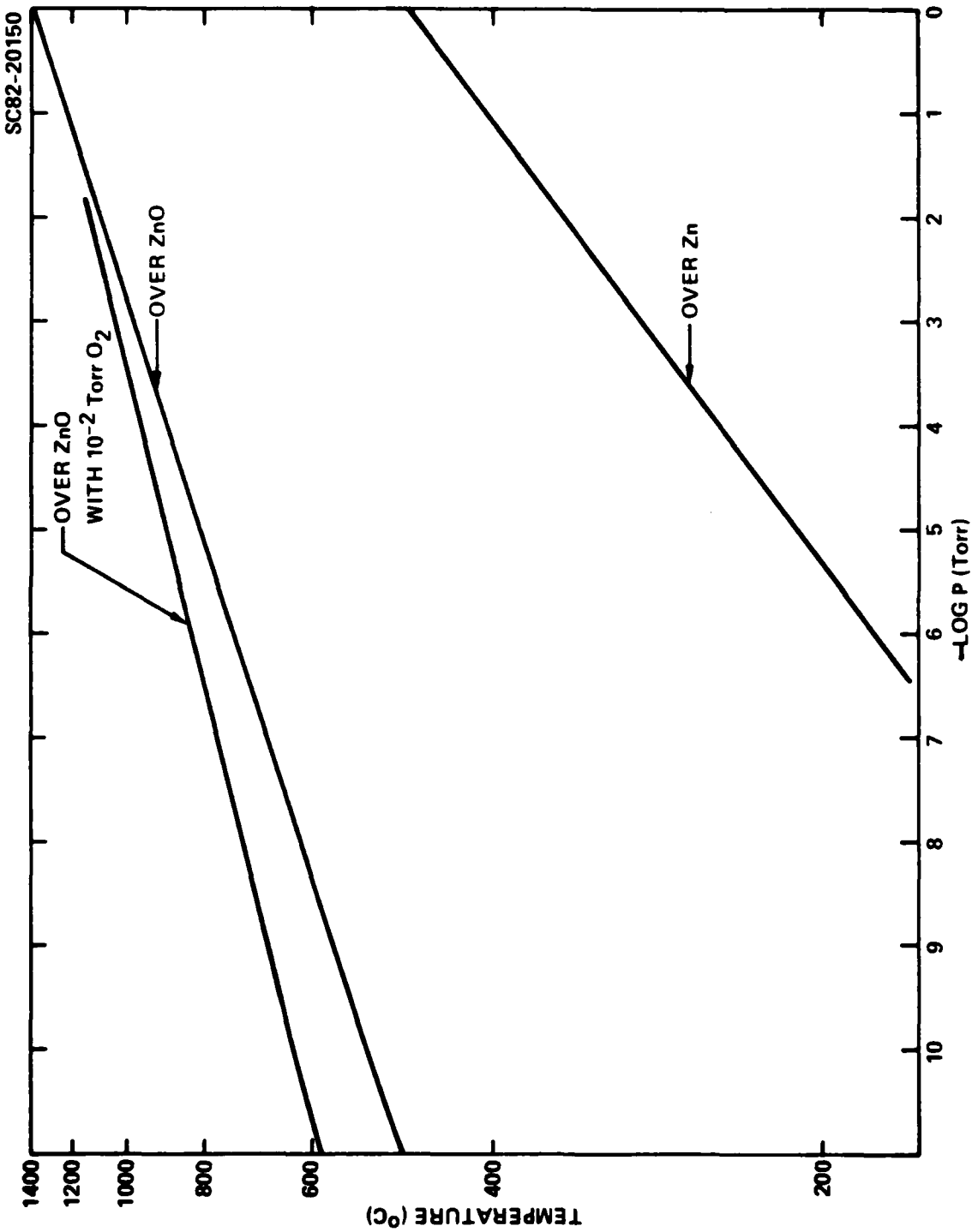

Fig. 10 Vapor pressure of Zn over ZnO and over Zn.

In another set of experiments, the ionization of the evaporant flux was measured. The experimental setup is shown in Fig. 11. Two large area electrodes flanked the pellet and were 2 cm apart and biased with respect to each other up to 250 Vdc. This bias was enough to deflect singly ionized species during their transit, even at high speeds of 10^5 cm/sec, corresponding to energies in eV range. Such high energies have been observed (R1) in laser evaporation of metals. The current sensitivity of the electrometer was 10^{-13} A. No current was detected during laser evaporation at any power level of laser beam. This puts an upper limit on the number of ionized species in the evaporant flux of 1 part in 10^{14}. The conclusion is that evaporated species are not ionized, as would be expected from particle energies at thermal evaporation temperatures. The above fact indicates that biasing the substrate during evaporation will not affect th velocity of the impinging species in the direction normal to the substrate.

3. Physics of ZnO Deposition

Experimental evidence indicates that the deposition of ZnO on the substrates proceeds by reactive evaporation of Zn with residual oxidizing gases in the vacuum environment. The oxidation of Zn proceeds rapidly due to exothermic nature of the reaction

$$Zn + \frac{1}{2} O_2 \rightarrow ZnO$$

for which the heat of reaction is $\Delta H = -83$ kcal/mole. If the oxidizing agent is N_2O or O_3, the energy of reaction is even more negative.

Zn atoms encounter few O_2 atoms, if any, during their transit form the source to the substrate in vacuum. However, the growth surface is bombarded by O_2 molecules at the rate predicted by kinetic gas theory. The Zn concentration on the surface is given by the arrival rate and reevaporation rate of Zn atoms. At growth temperatures higher than 200°C, the re-evaporation rate of Zn becomes comparable in order of magnitude to the impingement

SC82-20151

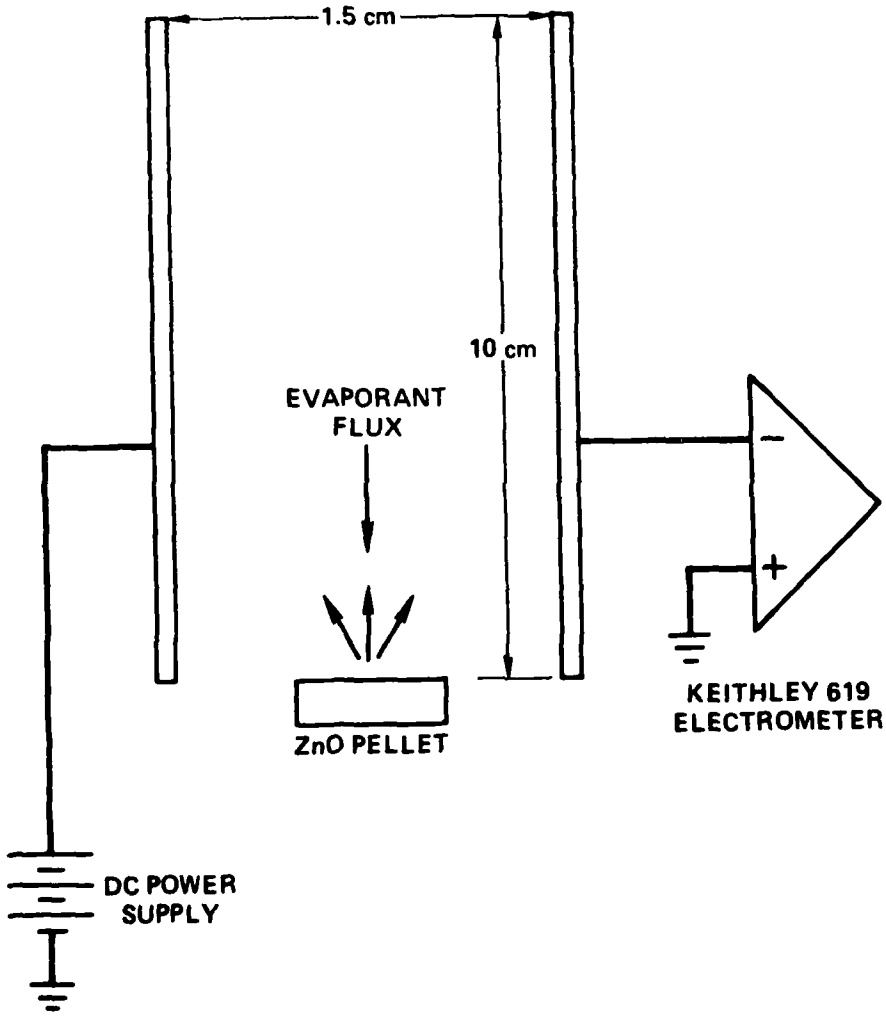

Fig. 11 Experimental set up to measure ionization during laser evaporation of ZnO.

rate from the source for a range of laser power levels used. In fact, at 200°C, the vapor pressure of Zn over solid Zn is $P_{Zn} \approx 10^{-5}$ Torr, hence evaporation rate, R_e

$$R_e = 44\sqrt{\frac{M_{Zn}}{T}}\ P(Zn) \times 10^{15}\ \text{atoms/cm}^2\text{-sec}$$

This corresponds to a few monolayesr/sec. The complete oxidation depends on the Zn and O_2 concentration on the surface and the reaction kinetics. If the ZnO evaporation rate is too rapid or if the reevaporation of Zn from the substrate surface is slow, as is the case at low substrate temperatures, the film grows Zn rich and will consist mostly of Zn or of Zn particles in ZnO matrix. In the case of Au substrates, the oxidation kinetics seems to be slowed, possibly due to alloying of Zn with Au.

4. Effects of Substrate

The crystallinity was found to depend on the type of substrate. The crystallinity was measured by x-ray diffraction (XRD) line peak height normalized by the thickness of the film.

For all substrates used, (0002) peak was the only x-ray diffraction line observed, indicating that the c-direction was normal to the substrate when the growth temperature was 250°C (Fig. 12). Sapphire, Si(100), Si(111), and Au(111) films used as substrates produced films with higher XRD counts. GaAs, quartz, thermal SiO_2 substrates produced films with lower crystallinity. The high crystallinity of films on c-sapphire is explained by the epitaxial growth of ZnO. However, there is no epitaxial relationship between ZnO and other substrates. The difference in crystallinity between different substrates is attributed to differences of adatom mobility. The fact that x-ray counts of films grown on quartz and thermal SiO_2 on Si are different also point out to the above conclusion. The film on Au substrates, where adatom mobility is expected to be highest, produced films with highest x-ray count.

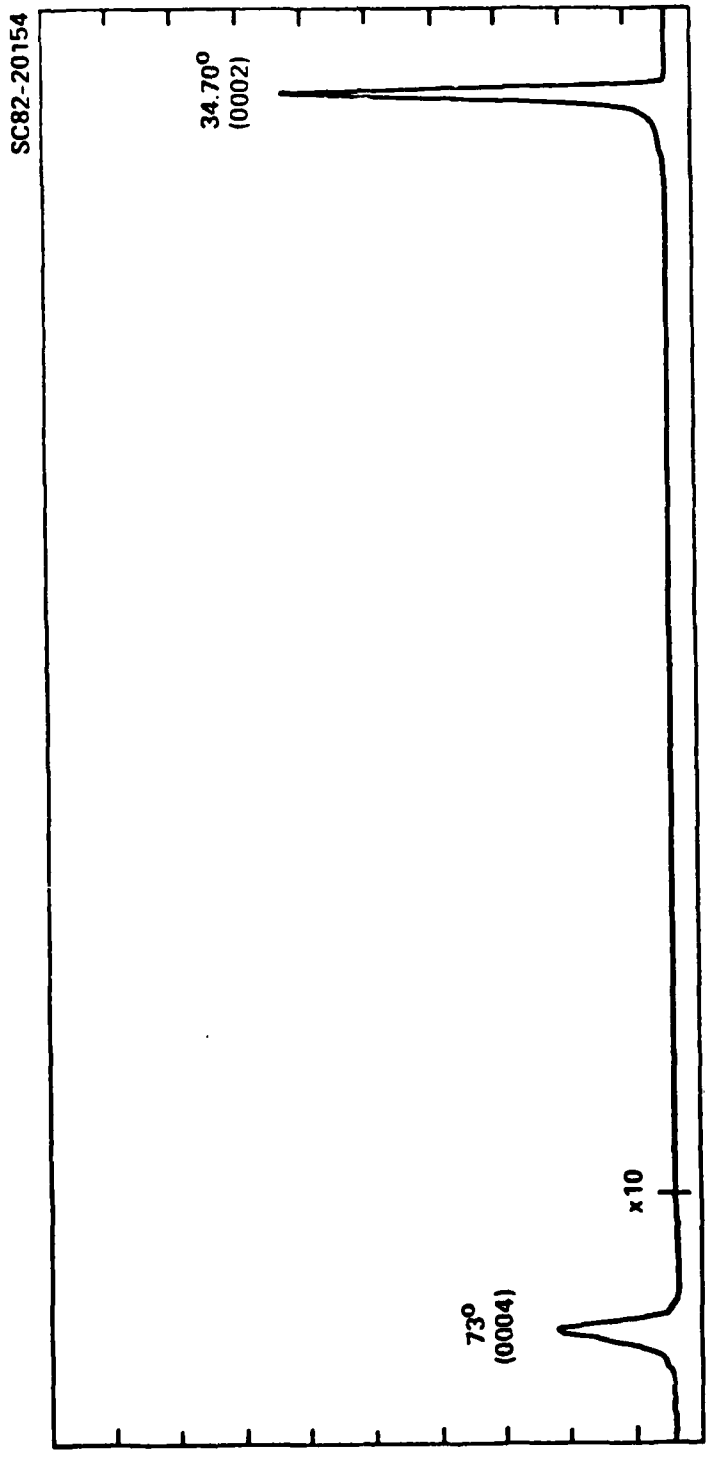

Fig. 12 X-ray diffraction pattern of a LADA ZnO film deposited on Si substrate at 250°C.

5. Effects of Temperature

The substrate temperature was found to have a strong effect on the growth rate, optical, and crystalline properties of ZnO films. Experiments were conducted with growth temperature ranging from 25°C to 450°C. In general, crystallinity increased (Fig. 13) and growth rate decreased with temperature. Temperature range for best crystalline structure was found to be 250°C-400°C. The increase in crystallinity is due to higher mobility of atoms, and the lower growth rate is thought to be due to re-evaporation of Zn atoms from the substrate surface or equivalently due to lowering of the sticking coefficient of Zn, as explained in Section 3.

Deposition on substrates at room temperature produced hard, glossy, black polycrystalline films. The transmittance and reflectivity spectra of these are shown in Fig. 14. The films are highly absorbing in the UV and visible range due to Zn precipitates. The polycrystals are not totally oriented, but (0002) XRD line is still the strongest peak. These films are truly ZnO as indicated by x-ray diffraction, as well as by ESCA measurements. Free Zn is not observed by either technique, although the black color of the films and the growth conditions indicate that Zn clusters or precipitates must exist in the bulk of the film.

Optically clear, highly crystalline and oriented films were produced at temperatures higher than 150°-200°C. The lower temperature bound for good quality films is affected by the evaporation rate as is explained in Sec. 3. In general, the films grown at temperatures higher than 400°C had lower crystallinity than films grown at 400°C.

6. Optical Properties

Transmission and reflectivity spectra for 1 μm thick film grown on quartz are shown in Fig. 15. The presence of interference maxima and minima indicates the uniform nature of the films. The refractive index values obtained from the position of the maxima and minima using the formula

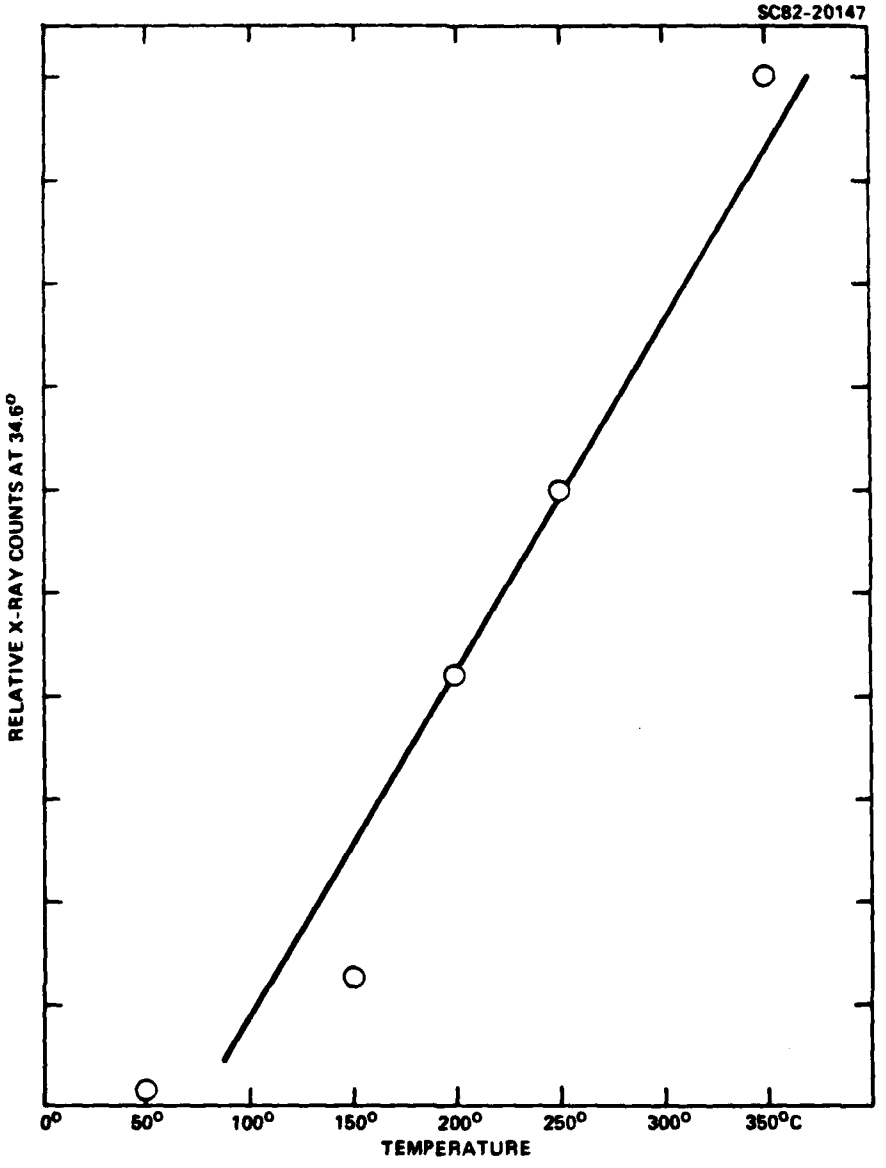

Fig. 13 Crystallinity (x-ray counts) vs growth temperature.

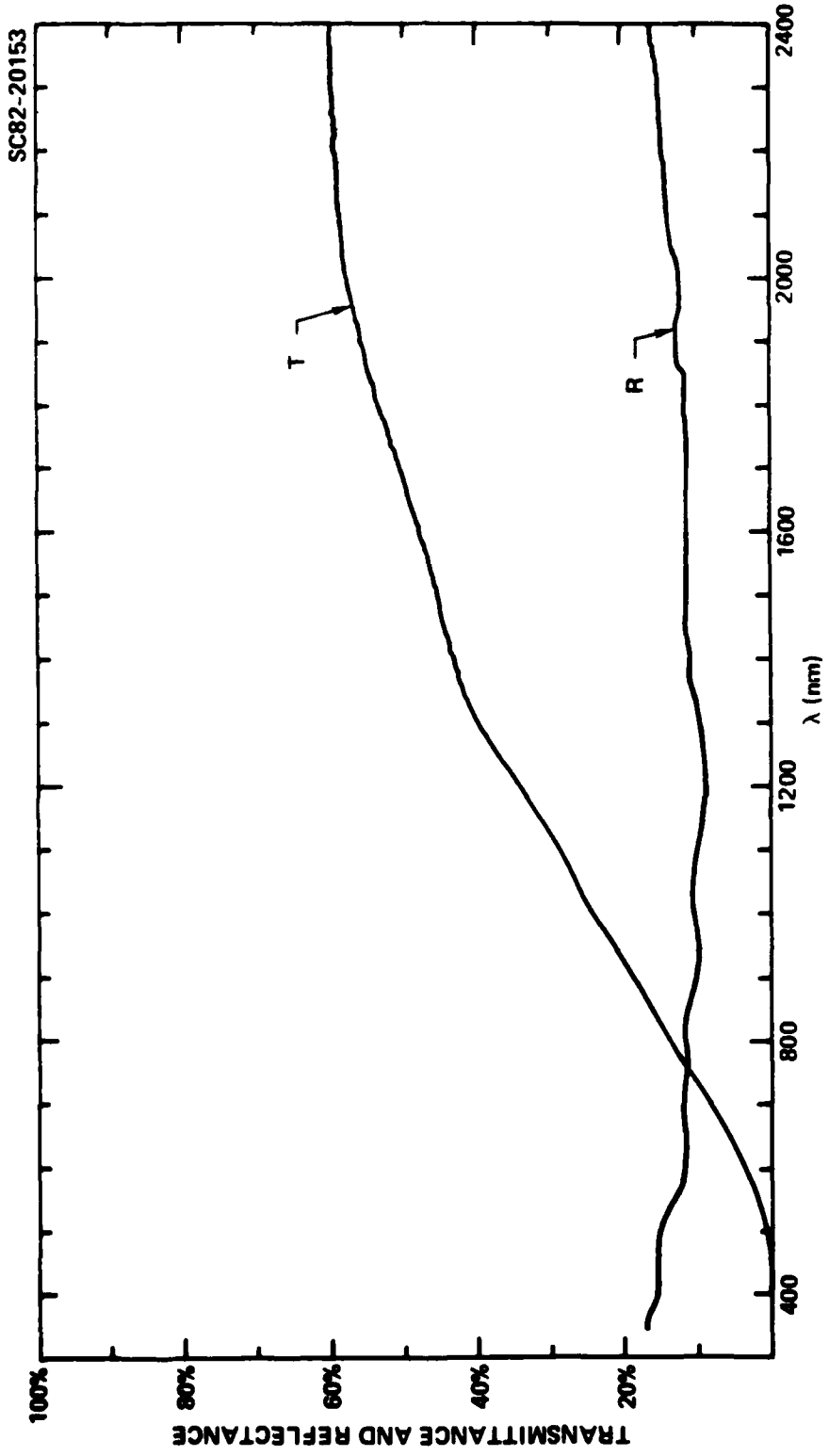

Fig. 14 Transmittance and reflectance spectra of a laser evaporated ZnO film on quartz substrate at room temperature.

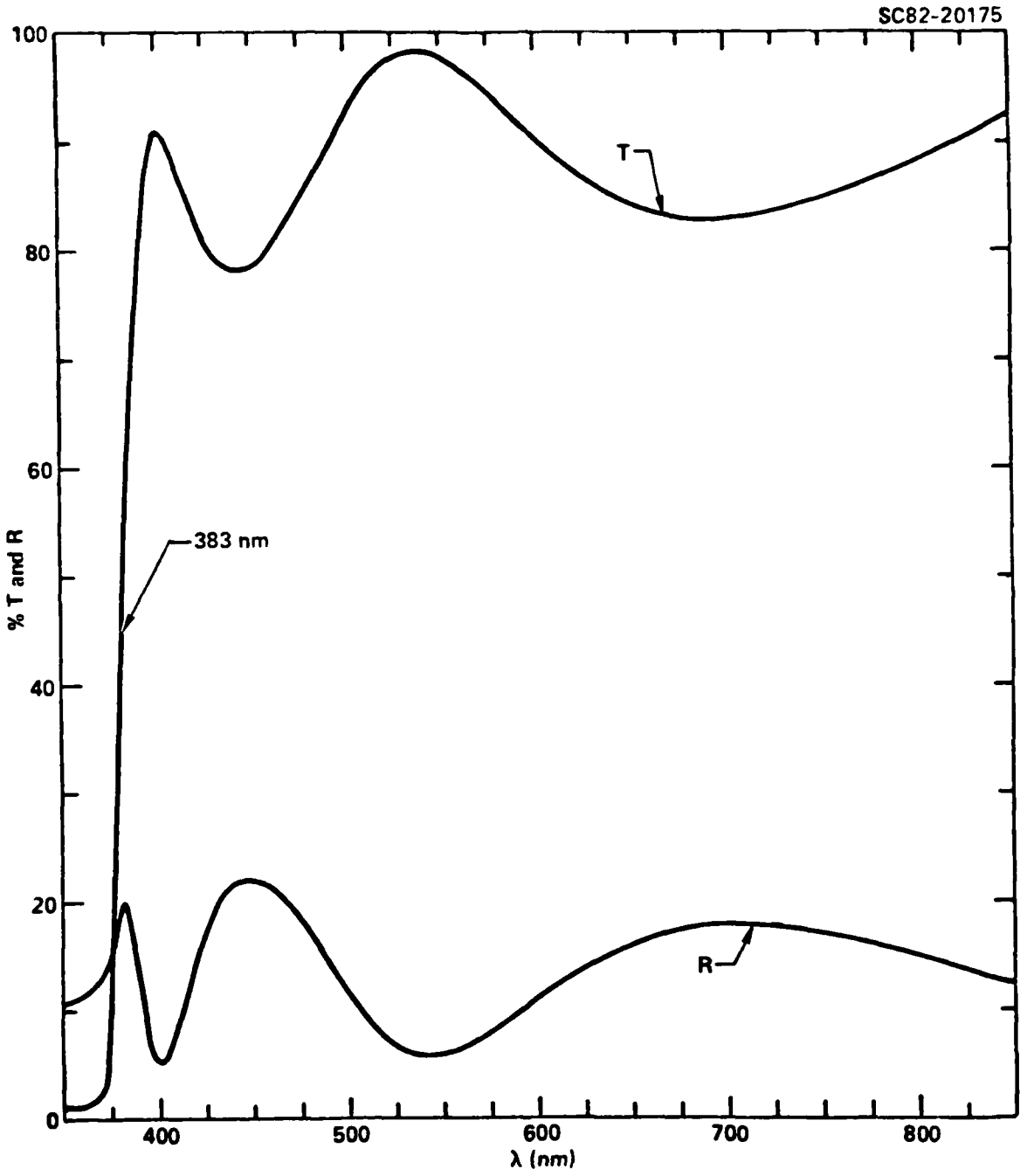

Fig. 15 Transmittance and reflectance spectra of a laser evaporated ZnO film on quartz substrate at 250°C.

$$n = \frac{1}{2t} \frac{\lambda_1 \lambda_2}{\lambda_1 - \lambda_2}$$

where t is the thickness and λ's are any adjacent maxima or minima, were found to be in close agreement with those obtained from ellipsometric measurements in the same films and refractive index values of best films obtained by RF sputtering as reported in literature.[4]

Samples grown on transparent quartz substrates were investigated optically by using polarizing plates under a microscope. This was to observe the orientation of grains utilizing the birefringent nature of ZnO. The samples appeared uniform, indicating that the grains were either too small so that any optical nonuniformities averaged out, or that the layer was nearly single crystal or an aggregate of crystallites similarly oriented in azimuthal direction. Laue Backreflection results favor the model of oriented polycrystallites aggregate.

7. Electrical Properties and Effect of Annealing

As-grown samples were found to be conducting with resistivity in the .1-1 Ω-cm range, as measured with van der Pauw method. Isothermal annealing in air or oxygen at temperatures of 250-700°C produced nonconducting films in the direction parallel to the film surface, but not across the film. This is thought to be due to the diffusion of oxygen along boundaries of columnar grains and the consequent increase of the potential barrier across the boundaries.[2] Thus, the conductivity parallel to the surface increases, whereas the conductivity in the direction normal to the surface is dominated by the bulk conductivity through the grains, thus it remains high.

8. Effect of Li Doping

The effect of Li doping on crystallinity and conductivity was investigated as a function of Li concentration in the source material. Li is known to compensate for native donors in ZnO.

In the initial set of experiments Li_2CO_3 powder was mixed with ZnO by

ball milling. The Li to Zn ratio in the source varied from 4%, 2%, 1%, 5%, .2%. The films grown with 1% or higher Li concentration were nonconducting, but had low or no crystalline structure. The films with low crystalline structure were under nonuniform stress as indicated by the high XRD line width and long trailing edge of the high angle side of the (0002) line.[3] Furthermore, the films were sensitive to ambient moisture and were observed to slowly deteriorate in room air. This is thought to be due to the excess Li in the films forming a basic solution with moisture in the environment, which then dissolves ZnO because of amphoteric nature of the latter. In fact, the ZnO:Li films were found to be water soluble and if left in DI water over a period of time, completely dissolved away. In another set of experiments, a water solution of $Li_2O \cdot H_2O$ was mixed with ZnO powder and the resulting sludge dried in vacuum. Since Li atoms are expected to be adsorbed on the surface of ZnO particles, it is expected that this technique would render a more uniform distribution of Li throughout the source material. This technique also allowed smaller amounts of the dopant to be used. The atomic Li concentration in the source varied from 1%-.1%. Films thus obtained were found to be nonconducting in the direction parallel and perpendicular to the film surface, but also to have excellent crystallinity. These were neither susceptible to ambient moisture nor dissolved in DI water. X-ray diffraction spectrum indicated that the films were stress free. The minimum amount of Li necessary to render the films highly resistive has not yet been determined. It is expected that further improvement in film quality will result when Li doping concentration is reduced.

9. Effect of O_2 Glow Discharge

Several LADA ZnO runs were made in a O_2 glow discharge environment. The O_2 pressure was held at 10 μm and AC glow discharge was obtained by means of high voltage electrical leads. The resulting films were transparent, had high resistivity, but poor crystallinity. The active O_2 in ionized or excited form is thought to completely oxidize the Zn atoms on the growth surface, thus eliminating free interstitial Zn that act as shallow donors. The poor

crystallinity, on the other hand, suggests the possibility of very small crystallites with potential barriers on their surfaces as the physical cause of high resistivity. Due to structural characteristics, we will use Li doped ZnO for high resistivity samples.

10. Effect of Gas in the Vacuum System

Most experiments have been carried out either in vacuum or in O_2 atmosphere at pressures of 5×10^{-4}, 1×10^{-3} and 1×10^{-2} Torr. No difference in optical, crystalline, electrical properties were observed in ZnO grown on quartz, Si, sapphire when the growth environment was hard vacuum (10^{-6} Torr) or O_2 gas at $5 \sim 10^{-4}$ Torr. However, ZnO grown on gold films in vacuum had scaly, black appearance, but became transparent, glossy-hard only when grown in O_2 atmosphere of 10^{-4} Torr pressure or higher. The above indicates that re-evaporation or oxidation kinetics is substrate dependent. Zn atoms on Au are slow to reevaporate or to oxidize, thus become buried under new layers of Zn and ZnO. This behavior is specific to Au and is not seen on Ti films. A possible explanation lies in the fact that Au and Zn form continuous alloys with 3 ordered phases (Fig. 16). The alloying of Zn on the surface may slow its oxidation because the solute Zn in low concentrations will behave somewhat like the solvent Au. Careful x-ray analysis did not show presence of Au_3Zn, AuZn or $AuZn_3$ compounds at the interface of ZnO and Au films.

Films grown in O_2 concentrations of $1\text{-}2 \times 10^{-2}$ Torr on any substrate showed poor crystallinity but low resistivity. It is to be noted that 10^{-20} Torr O_2 pressure with glow discharge gave films with equally poor crystallinity, but very high resistivity and high breakdown voltage as explained in Section 9.

11. Effect of Annealing

Isothermal annealing affects optical, electrical, and crystalline properties of films. In general, crystallinity improved with annealing

SC82-20148

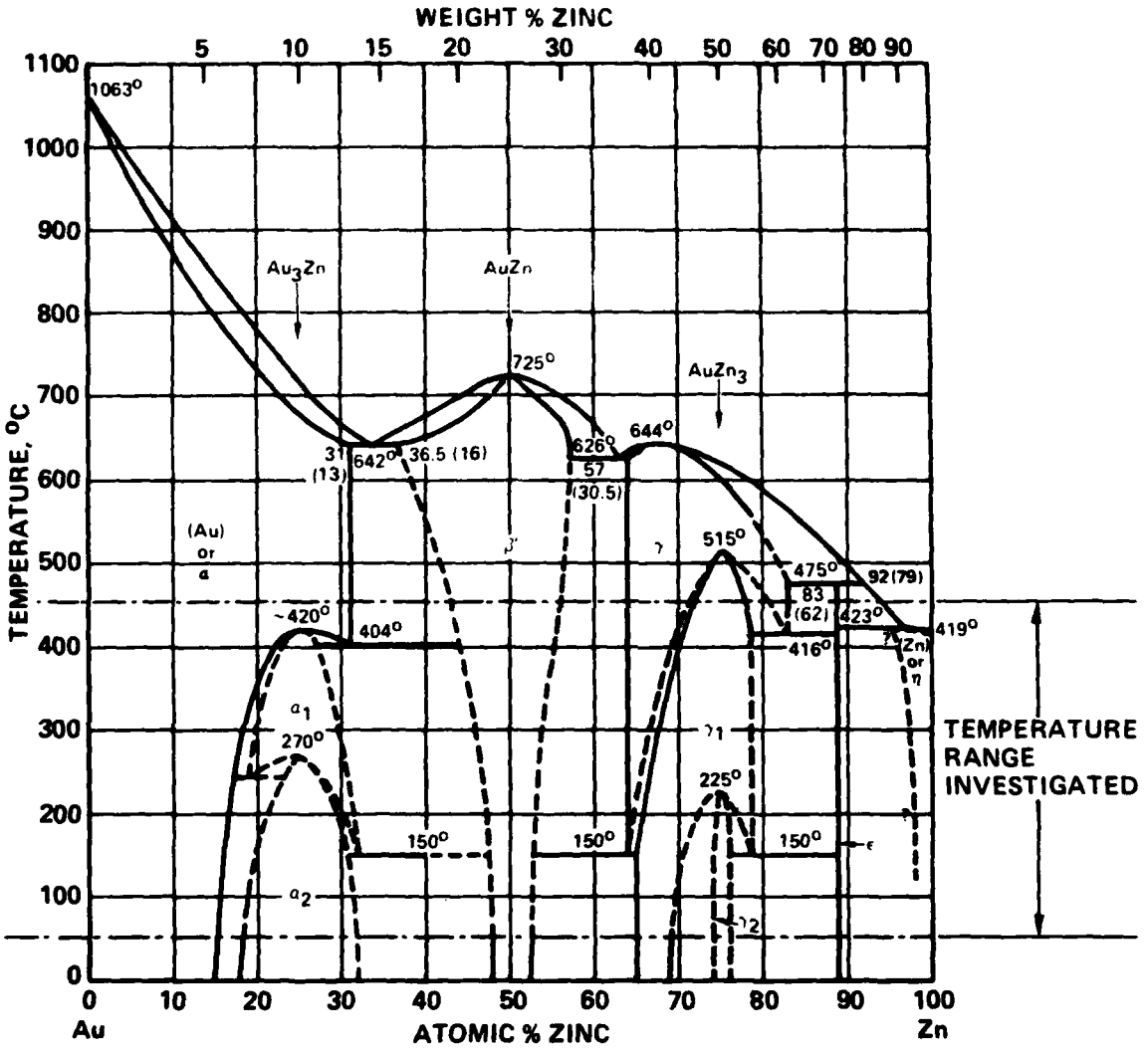

Fig. 16 Phase diagram of Au-Zn system.

temperatures of 250°-400°C and with annealing time within 2 hours. However, when film structure was so disordered that no crystalline order exists, annelling does not improve crystallinity. Isothermal annealing at 250°C in flowing O_2 for 8 hours hardened the films, eliminating low breakdown regions. Annealing at higher temperatures 400°-700°C changed the black-glossy films grown at room temperature to transparent or translucent films, possibly by dissolving or oxidizing Zn clusters that give rise to the dark color the films.

Problems and Future Plans

The development on LADA ZnO will continue with special emphasis on obtaining higher device quality material. Since amount of dopant Li in the film bears a direct relationship with crystallinity and other chemical properties, an effort to investigate the minimum Li doping to give high resistivity and breakdown voltage in the films will be made. Other growth parameters (e.g. temperature, residual gas, substrate cleanliness, etc.) will be optimized using the material with optimum Li concentration.

ZnO films will be grown on quartz and on thermal oxide on Si, with Gigaherz range SAW pattern metallization. These samples will be evaluated to measure the electrochemical coupling coefficient and attenuation losses.

3.0 REFERENCES

1. J. F. Friichtenicht, Rev. Sci. Inst. 45, 51 (1974).
2. J. C. Yen, J. Vac. Sci. Tech. 12, 47 (1975).
3. M. Miijra, Jap. J. App. Phys. 21, 264 (1982).
4. J. R. Shealy, et al J. Electrochem. Soc. 128, 558 (1981).

DISTRIBUTION

Director
Defense Advanced Research
Project Agency
1400 Wilson Blvd.
Arlington, VA 22209

Attn: Program Management (2)
Attn: Sven Roosild (1)

Director
Night Vision & Electro-Optics
Laboratory
NV&EOL-RD
Fort Belvoir, VA 22060

Attn: Mr. William Guiterrez (1)

Defense Technical Information Center (12)
Cameron Station
Alexandria, VA 22314

Science Center Distribution:

J.T. Longo (1)
M. Khoshnevisan (1)
J.T. Cheung (1)
Group Secretary (2)
C&P-Data Management (1)
Library Original + (1)
H. Sankur (1)
D.T. Cheung (1)